RSC Medicinal Chemistry

ROYAL SOCIETY OF CHEMISTRY

RESEARCH ARTICLE

Cite this: *RSC Med. Chem.*, 2022, **13**, 175

Design, synthesis, and biological evaluation of C_6-difluoromethylenated epoxymorphinan Mu opioid receptor antagonists†

Andrew J. Kassick,[ab] Anny Treat,[c] Nestor Tomycz,[b] Michael G. Feasel,[d] Benedict J. Kolber[c] and Saadyah Averick *[ab]

Received 24th August 2021,
Accepted 28th October 2021

DOI: 10.1039/d1md00285f

rsc.li/medchem

The recent widespread abuse of high potency synthetic opioids, such as fentanyl, presents a serious threat to individuals affected by substance use disorder. Synthetic opioids generally exhibit prolonged *in vivo* circulatory half-lives that can outlast the reversal effects of conventional naloxone-based overdose antidotes leading to a life-threatening relapse of opioid toxicity known as renarcotization. In this manuscript, we present our efforts to combat the threat of renarcotization by attempting to extend the half-life of traditional MOR antagonists through the design of novel, fluorinated 4,5-epoxymorphinans possessing increased lipophilicity. Analogues were prepared *via* a concise synthetic strategy highlighted by decarboxylative Wittig olefination of the C_6 ketone to install a bioisosteric 1,1-difluoromethylene unit. C_6-difluoromethylenated compounds successfully maintained *in vitro* potency against an EC_{90} challenge of fentanyl and were predicted to have enhanced circulatory half-life compared to the current standard of care, naloxone. Subsequent *in vivo* studies demonstrated the effective blockade of fentanyl-induced antinociception in mice.

Introduction

Synthetic mu opioid receptor (MOR) agonists constitute an important class of biologically relevant small molecules that exhibit both interesting chemical diversity and clinical utility. Among the most notable of the various MOR agonist structure classes is the highly potent 4-anilidopiperidine series of synthetic opioids comprised of the schedule II prescription pain reliever fentanyl (**1**) and its related analogues. Developed by Janssen and coworkers from the requisite 4-phenylpiperidine pharmacophore present in morphine and other 4,5-epoxymorphinan congeners (Fig. 1),[1] the 4-anilidopiperidines display high intrinsic lipophilicity relative to morphine that is manifested in their ability to more rapidly permeate the blood brain barrier (BBB) and strongly activate the MOR at low nanomolar concentrations resulting in powerful anesthetic and analgesic properties. Despite being effective therapies for the management of both acute and chronic severe pain with *in vivo* potencies over 100-fold greater than morphine,[2,3] fentanyl and its derivatives remain notorious for their serious and potentially fatal addictive and respiratory depressive effects that have ultimately given rise to the current epidemic of opioid-induced overdoses and deaths that has plagued the United States (US) for nearly a decade. While this crisis initially impacted the US, the effects of the opioid epidemic now extend internationally as rising opioid-related mortalities from the pervasive abuse of fentanyl and other synthetic opioids have been reported throughout Canada, Europe, and Australia.[4–7]

To combat the effects of synthetic opioid-induced overdose, medical professionals and first responders have relied extensively on the clinically approved MOR antagonist naloxone (Narcan®, **2**); however, the efficacy of this opioid reversal agent has been seriously challenged by fentanyl and other

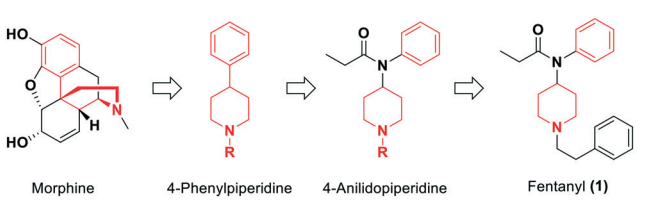

Fig. 1 Evolution of fentanyl and the 4-anilidopiperidine chemotype from the 4-phenylpiperidine pharmacophore of morphine.

[a] *Neuroscience Disruptive Research Lab, Allegheny Health Network Research Institute, Allegheny General Hospital, Pittsburgh, PA 15212, USA. E-mail: saadyah.averick@ahn.org*
[b] *Neuroscience Institute, Allegheny Health Network, Allegheny General Hospital, Pittsburgh, PA 15212, USA*
[c] *Department of Neuroscience and Center for Advanced Pain Studies, University of Texas at Dallas, Richardson, TX 75080, USA*
[d] *Research and Technology Division, DEVCOM Chemical Biological Center, Aberdeen Proving Ground, MD 21010-5424, USA*

† Electronic supplementary information (ESI) available. See DOI: 10.1039/d1md00285f

highly potent 4-anilidopiperidines. This limited capacity of naloxone to effectively reverse severe respiratory depression associated with synthetic opioid toxicity has been attributed in large part to the high lipid solubility exhibited by fentanyl-based MOR agonists. The characteristic lipophilicity of 4-anilidopiperidine opioids leads to their rapid crossing of biological membranes such as the blood brain barrier (BBB) and facilitates their absorption into adipose tissue effectively shielding these compounds from metabolism and artificially extending their *in vivo* circulatory half-lives. Evidence of the prolonged circulatory half-life of fentanyl (8–10 h) has been documented in clinical studies.[8–10] In contrast, naloxone possesses a significantly lower degree of lipophilicity relative to fentanyl and its analogues and is not taken up into adipose tissue. As a result, it undergoes rapid phase II metabolism and deactivation by the liver isozyme UDP glucuronosyltransferase 2B7 (UGT2B7) to form the corresponding hydrophilic conjugate, naloxone-3-glucuronide which is promptly cleared leading to the distinctive short half-life of naloxone (~1 h). This pharmacokinetic disparity between naloxone and synthetic opioids poses a serious threat to individuals affected by substance use disorder as it can lead to a potentially life-threatening phenomenon known as renarcotization where overdose victims re-succumb to the toxic effects of residual opioids following the rapid metabolism and clearance of a therapeutic dose of naloxone. Prevention of this condition often times requires the administration of larger or repeated doses of naloxone;[11–13] however, this treatment strategy can precipitate undesirable opioid withdrawal symptoms.[14,15] As a result, new medications or longer-lasting formulations of existing opioid reversal agents are needed to more effectively treat overdose in opioid dependent individuals and others at risk of accidental exposures to synthetic opioids.

In an attempt to address this critical need, we sought to increase the *in vivo* circulatory half-lives of currently employed MOR antagonists by preparing novel derivatives that incorporate fluorine atoms into the parent scaffolds (Fig. 2). Fluorine substitution has the potential to afford increases in lipophilicity that can give rise to enhancements in metabolic stability and other physicochemical properties including permeability across biological membranes, leading to better absorption and bioavailability.[16,17] In some cases, enhancements in the binding affinity of a compound to its target protein have also been observed.[16,17] As a result, we have designed and synthesized analogues of the classical opioid reversal agents naloxone, naltrexone, and nalmefene that bear a 1,1-difluorinated olefin moiety, a known carbonyl bioisostere,[18–20] at the C_6 position of the antagonist core structure (Fig. 2). It was envisioned that the requisite difluoroolefin could be readily accessed in a single chemical step from commercially available starting materials to arrive at the desired MOR antagonist analogues 6-CF_2-NLX (**5**) and 6-CF_2-NTX (**6**). This modification was anticipated to result in a corresponding increase in hydrophobicity of the epoxymorphinan scaffold and arrive at compounds similar to fentanyl with regard to its ability to permeate and remain in tissues thus attenuating antagonist metabolism and improving circulatory half-life. Moreover, the minor structural change imparted to the molecular framework of these compounds as a result of the introduction of sterically small fluorine atoms was also believed to have little effect on their overall antagonist profile and *in vivo* potency thus allowing for the maintenance or possible enhancement of the pharmacological activity exhibited by naloxone, the current standard of care for the reversal of opioid intoxication. Herein we report our results toward the synthesis and biological evaluation of novel, C_6-difluoromethylenated epoxymorphinan MOR antagonists that demonstrate increased lipophilicity while maintaining *in vitro* potency against an EC_{90} challenge of fentanyl and *in vivo* potency against the anti-nociceptive effects of high dose fentanyl in mice.

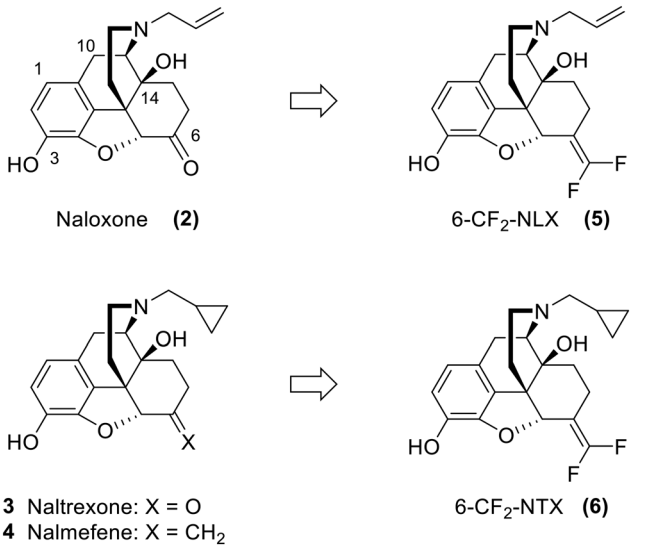

Fig. 2 Clinically approved opioid reversal agents naloxone (**2**), naltrexone (**3**), and nalmefene (**4**) and their corresponding C_6-difluoroolefin analogs.

Experimental section

Materials and methods

Synthetic chemistry materials. Naloxone hydrochloride dihydrate and naltrexone hydrochloride were purchased from Sigma-Aldrich (St. Louis, MO) and Alfa Aesar (Ward Hill, MA), respectively, and subsequently converted to the corresponding free bases *via* acid–base extraction with saturated aqueous sodium bicarbonate ($NaHCO_3$). Anhydrous dichloromethane (CH_2Cl_2), dimethylformamide (DMF), and methanol (CH_3OH) were purchased from Sigma-Aldrich (St. Louis, MO). Water was purified *via* a Millipore Synergy water purification system. [Tris(dimethylamino)phosphonio]difluoroacetate **9** was prepared from ethyl bromodifluoroacetate and tris(dimethylamino)phosphine, sourced from Sigma-Aldrich (St. Louis, MO), according to the literature procedure.[21] All other reagents and solvents were used as received unless otherwise noted.

Pharmacological assaying materials. Hank's Balanced Salt Solution (1X), cell growth media (Ham's F-12, MEM Non-Essential Amino Acids Solution, FBS, and G418 selective antibiotic), non-enzymatic dissociation solution (Versene™ Solution), and HEPES were purchased from Invitrogen (Gathersburg, MD). Naloxone, forskolin and IBMX were purchased from Sigma-Aldrich (St. Louis, MO). Fentanyl citrate was purchased through Mallinckrodt Pharmaceuticals (St. Louis, MO). Optiplate 384 white opaque 384-well microplates, TopSeal™-A adhesive film, and the Lance Ultra cAMP kit were purchased from Perkin Elmer (Waltham, MA). Chinese Hamster Ovary (CHO) K1 cells, CHO-K1 cells (Charles River Laboratories Wilmington Massachusetts) stably expressing the human mu opioid receptor gene (OP3; MOR) were purchased/licensed from ChanTest Corporation, now Charles River Laboratories (Wilmington, MA). ^{1}H, ^{13}C, and ^{19}F NMR spectra were measured in DMSO-d_6 on a Bruker Avance 500 MHz spectrometer. ^{1}H NMR chemical shifts are reported in ppm employing the residual solvent resonance as the internal standard (DMSO: δ 2.50 ppm). LC-MS analysis was performed on a Dionex Ultimate 3000 uHPLC system coupled to a Thermo Scientific TSQ Quantum Access MAX triple quadrupole mass spectrometer. Reverse-phase chromatographic separation was accomplished on an Agilent ZORBAX Eclipse Plus C18 column (3.5 μm, 100 × 4.6 mm) with acetonitrile (CH_3CN) and water (H_2O), modified with 0.1% formic acid, as the mobile phase solvents. Standard HPLC method consisted of a linear gradient from 20–95% CH_3CN over 5 min followed by a hold at 95% CH_3CN for 1 min and then a re-equilibration at 20% CH_3CN for 2.5 min. (Total run time: 10 min, flow rate: 0.400 mL min^{-1}, injection volume: 10 μL).

Cell culture and transfections. CHO-K1 cells expressing the human MOR were cultivated in Ham's F12 medium, supplemented with 10% FBS, 1× NEAA for 24 h post-thaw, and media replaced at 24 h by similar media with 0.4 mg mL^{-1} Geneticin (G418) selection antibiotic until ready to assay. Subconfluent cells (~70%) were used for the assay.

Lance ultra cAMP assay. The competitive binding assay procedure was followed exactly as described in the manufacturer's Assay Development Guidelines for assessing antagonism. In brief, on the day of the assay, ligand solutions (10 mM stocks in DMSO) were diluted into assay buffer and added to the wells of a 384-well Optiplate in triplicate. Cell suspensions (1000 cells per well) were added and subsequently treated with EC_{90} doses of fentanyl (data not shown) and log-doses of the various MOR antagonists (naloxone, 6-CF_2-NLX, and 6-CF_2-NTX) spanning 10^{-4} – 10^{-14} M. The test compounds were then incubated for 30 minutes at ambient temperature along with a null control group of untreated cells (no antagonist). Following incubation, freshly prepared lysis buffer containing assay tracer (Eu-cAMP) and antibody (Ulight™- anti-cAMP) was added and the microplate was covered by adhesive film prior to a second incubation in the dark for 1 h at ambient temperature. The plate was then read on a Molecular Devices FlexStation III by exciting the wells with light of 340 nm and measuring the emission at 615 and 665 nm.

Animals. Male and Female C57Bl/6 J mice (32 total), ranging from 10–12 weeks of age, were housed in 12 h light/dark cycle and food and water were made available *ad libitum*. All testing was performed during the light-on cycle of the animals in a room separate from their original housing location, food and water were available *ad libitum* between tests. The testing room was maintained at 21.5 ± 0.5 °C. White noise (~55 dB) was used to drown out any sounds from adjacent rooms. All animals were acclimated to the room for at least 1 h prior to testing, and to the experimenter for at least 30 minutes prior to testing.

Animal use ethical statement

All mouse procedures were performed in accordance with the Guidelines for Care and Use of Laboratory Animals of The University of Texas at Dallas (protocol 20-04) and approved by the Institutional Animal Care and Use Committee at the University of Texas at Dallas.

***In vivo* drugs.** Fentanyl citrate (Spectrum Chemicals, New Brunswick, NJ) was dissolved in 0.9% saline (at a concentration of 0.04 mg mL^{-1}) and the volume of injection was determined by the weight of the animal to achieve a dose of 0.4 mg kg^{-1} per animal (*e.g.* a 20 g mouse received 200 μL of fentanyl citrate solution). Naloxone hydrochloride (Sigma) and hydrochloride formulations of 6-CF_2-NLX (**5**) and 6-CF_2-NTX (**6**) were dissolved into phosphate buffered saline containing 10% DMSO at a concentration of 1 mg mL^{-1} and the volume of injection was determined by the weight of the animal to achieve a dose of 10 mg kg^{-1} per animal (*e.g.* a 20 g mouse received 200 μL of treatment).

Hotplate thermal assay. Thermal algesia was tested on a hotplate apparatus consisting of a 10 × 16 cm thermoelectric plate (TE technology CP-061HT) connected to a temperature controller (TE technology TC-48-20). A mobile, transparent, and colorless plexiglass rectangular box (10 × 16 × 25 cm) was placed on the hotplate to form the observation area. Adult male and female mice first received acclimations to the hotplate apparatus while it was set to a non-noxious temperature (one trial 10–30 minutes prior to the baseline test, and two acclimation trials 24 h before test day). Acclimation trials were performed with the hotplate maintained at 31 ± 0.5 °C for approximately 60 s per trial. Following acclimation, baseline tests (48 h before drug or vehicle administration) and post treatment hotplate tests (1, 8, and 24 h post vehicle, naloxone or compound treatment) were performed. For the baseline and post treatment tests, the metal hot plate was maintained at 49 ± 0.5 °C. 48 h after the baseline hotplate measurement, and 24 h after receiving two additional acclimation trials, mice received subcutaneous injections (180–290 μL, depending on the weight of the animal) on their dorsal side of either vehicle (10% DMSO, 90% phosphate buffered saline), 10 mg kg^{-1} naloxone, 6-CF_2-NLX (**5**) and 6-CF_2-NTX (**6**). One, eight, and twenty-four hours post treatment, each mouse received an intraperitoneal injection (180–290 μl, depending on the weight of the animal) of 0.4 mg kg^{-1}

fentanyl. Latency on the hotplate was measured 15 minutes post fentanyl injection. Measurements were made by placing one mouse on the hotplate at a time and recording the response latency with a stopwatch to the nearest 0.01 s. A cut-off latency of 30 s was used. Pain-associated behaviors were typified as either licking of the hind-paw or jumping. After each measurement, the plate was wiped clean of all urine and feces. The maximum possible effect (% MPE) of fentanyl treatment was calculated using the following formula: % MPE = "test day (s) – baseline (s)"/"30 s – baseline" × 100%. All experimenters were blinded to experimental drug treatment during testing and scoring.

Data Analysis & Statistics. The measured fluorescence energy transfer ratio (665 nm/615 nm) was plotted against antagonist concentration in GraphPad Prism v8.3.0 (San Diego, CA) and normalized to the control antagonist's (naloxone) response. Concentration-response curves were fitted by nonlinear regression [antagonist] *vs.* response – three parameter. For the hotplate assays, groups were compared to one another at the one hour, eight hour, and twenty-four hour time points using One-way ANOVA with Tukey *post-hoc* analysis. The potential for sex differences in the hot plate assay was not statistically analyzed as the study was not powered to detect sex differences. P values <0.05 were considered statistically significant.

Results and discussion

In silico modeling of Log P and pharmacokinetics

To explore the feasibility of our proposed fluorinated derivatives to mimic the heightened tendency of fentanyl and related analogues to permeate the BBB and partition into the highly nonpolar environment of adipose tissue, we initially conducted *in silico* modeling studies to quantitatively assess the lipophilicity of C_6-difluoromethylenated compounds 6-CF_2-NLX (**5**) and 6-CF_2-NTX (**6**). Lipophilicity, commonly expressed as Log P, has long been recognized as a valuable parameter for predicting many other physicochemical and ADME/Tox properties of bioactive molecules ranging from solubility and permeability to distribution and metabolism.[22–26] Given the well documented correlation that exists between lipophilicity and BBB permeation,[26–28] it was envisioned that a significant increase in Log P for the difluorinated compounds would translate into more rapid brain tissue distribution leading to attenuated metabolism and a corresponding enhancement in circulatory half-life. Such improvements could ultimately arrive at longer lasting MOR antagonists capable of more effectively combating their synthetic opioid agonist counterparts.

Log P estimations for difluorinated analogues 6-CF_2-NLX (**5**) and 6-CF_2-NTX (**6**) were calculated based on two separate methods within MedChem Designer v.5.0.0.4 (Simulation Plus, Lancaster, CA). The resulting Moriguchi (MLog P) and Simulations Plus (S + Log P) predictions of partitioning values are indicated in Table 1. As anticipated, the introduction of fluorine atoms at the C_6 position of the parent epoxymorphinan scaffold resulted in higher predicted Log P values relative to currently employed MOR antagonists suggesting that 6-CF_2-NLX (**5**) and 6-CF_2-NTX (**6**) should exhibit a greater ability to penetrate and remain in brain and adipose tissue as these *in silico* lipophilicity values more closely resemble the Log P of the hydrophobic MOR agonist, fentanyl (Log $P_{fentanyl}$ = 3.82).[29]

Table 1 Calculated molecular weights and predicted Log P for traditional epoxymorphinan MOR antagonists and experimental hydrophobic derivatives

Compound	Molecular weight	Moriguchi estimation of Log P	Simulations plus model of Log P
Naloxone	327.383	2.038	1.199
Naltrexone	341.410	2.352	1.601
Nalmefene	339.430	3.363	2.473
6-CF_2-NLX	361.391	3.277	2.631
6-CF_2-NTX	375.418	3.581	3.043

Further support for the prospect of longer lasting MOR antagonists *via* fluorine atom incorporation was obtained through the application of physiologically based pharmacokinetic (PBPK) modeling.[30,31] Recent advances in predictive software design have resulted in PBPK simulations becoming more widely utilized by the pharmaceutical industry for drug discovery and development as well as the regulatory submission process.[31] In the present study, PBPK computational models provided simulations of human pharmacokinetics (PK) in both plasma (Fig. 3) and the brain (Fig. 4 and 5) for naloxone, 6-CF_2-NLX (**5**), and 6-CF_2-NTX (**6**) employing GastroPlus v.9.6.0001 PBPK modeling software (Simulations Plus, Lancaster, CA). For the brain, both kinetics and area under the curve (AUC) were modeled to assess drug accumulation relative to the benchmark compound naloxone. The physiology modeled in these simulations was that of a 30-year old human male (American) weighing 86.27 kg (Fig. S1†) employing a nominal 4 mg IV bolus dose of test compound. PK predictions followed a 24 h post-injection time course as illustrated in the corresponding concentration-time profiles. All predictions were based purely on the two-dimensional (2D) structure of the compounds with no experimental data

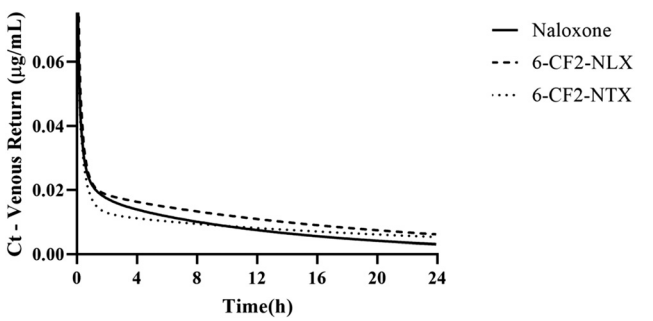

Fig. 3 Modeled pharmacokinetics in the blood plasma for naloxone and C_6-difluoromethylenated compounds **5** (6-CF_2-NLX) and **6** (6-CF_2-NTX). Simulation shows plasma concentrations over 24 h after an IV bolus dose of 4 mg of each drug.

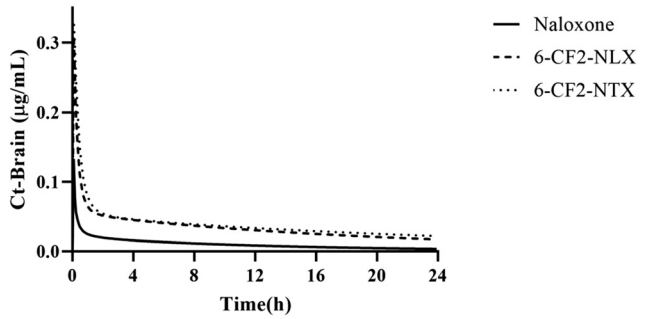

Fig. 4 Modeled pharmacokinetics in the brain tissue for naloxone and C_6-difluoromethylenated compounds **5** (6-CF_2-NLX) and **6** (6-CF_2-NTX). Simulation shows plasma concentration over 24 h after an IV bolus dose of 4 mg of each drug.

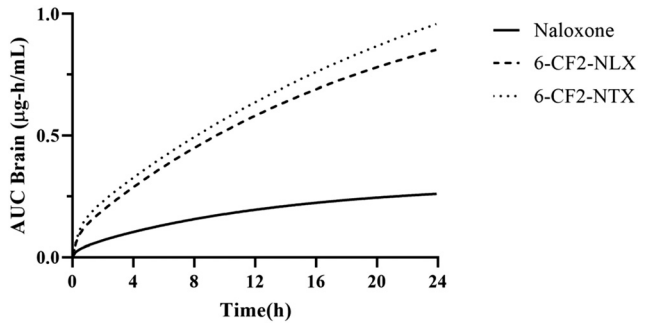

Fig. 5 Drug accumulation modeled in the brain over 24 h after an IV bolus of 4 mg of each of three drugs.

populated into the model. All properties were derived from ADMET Predictor v.8.1.0.0 (Simulations Plus, Lancaster, CA).

Our PBPK modeling efforts predicted that 6-CF_2-NTX (**6**) would demonstrate the most rapid redistribution from plasma followed by the slowest elimination clearance of all compounds tested (Fig. 3). Brain kinetics data presented in Fig. 4 indicate that 6-CF_2-NTX (**6**) should also partition more readily into the CNS and remain there longer than naloxone potentially allowing for the more effective MOR blockade of fentanyl. In addition, PBPK simulations estimate that 6-CF_2-NTX (**6**) would exhibit the highest cumulative amount of drug distributed into the CNS (Fig. 5). 6-CF_2-NLX (**5**) is predicted to have higher plasma concentrations over the 24 h simulation with slower redistribution than both naloxone and 6-CF_2-NTX while achieving similar brain concentrations as 6-CF_2-NTX, translating into a drug compound with slower onset but that displays similar brain penetration and is longer lasting relative to naloxone. As depicted in Fig. 5, 6-CF_2-NLX (**5**) also achieves slightly less accumulation in the CNS over the 24 h model compared to naltrexone analogue (**6**). Naloxone, on the other hand, displays markedly lower brain accumulation relative to its fluorinated counterparts that ultimately levels off as an indication that no additional naloxone is reaching the brain. These computational models would suggest that 6-CF_2-NLX (**5**) is characterized by a slower onset therapeutic effect; however, once in the brain, its hydrophobic character promotes brain tissue sequestration that may extend its circulatory half-life and potentially allow for a more effective antidote. Overall, the initial LogP calculations and PBPK simulations of human pharmacokinetics in both plasma and the central compartment provided support for the synthesis and further biological evaluation of difluorinated analogues 6-CF_2-NLX (**5**) and 6-CF_2-NTX (**6**) in an attempt to improve the central distribution as well as tissue-specific duration of the clinically approved opioid reversal agent naloxone.

Chemistry

Difluoromethylenated analogues **5** and **6** were prepared according to the three-step reaction sequence outlined in Scheme 1. Selective protection of the phenolic hydroxyl moiety in both naloxone and naltrexone with benzoyl chloride and triethylamine afforded the corresponding benzoate esters **7** and **8** in excellent yield.[32] Installation of the requisite 1,1-difluoromethylene group was then accomplished *via* decarboxylative Wittig olefination of the C_6 ketone residue present in the parent epoxymorphinan scaffolds with a phosphonium ylide derived from [tris(dimethylamino)phosphonio]difluoroacetate **9** at elevated temperature.[21] The low isolated yield obtained from this reaction can be attributed to a complex product mixture resulting from unwanted side-reactivity of the nonactivated, enolizable ketone substrate at the prescribed reaction temperature coupled with difficult chromatographic separation. Subsequent benzoate hydrolysis of compounds **10** and **11** with K_2CO_3 in methanol at ambient temperature then furnished the desired difluoro MOR antagonist analogs **5** and **6** in 67% and 71% yield, respectively.

In vitro MOR antagonist potency against fentanyl challenge

Our evaluation of the *in vitro* potency for novel, difluorinated MOR antagonist analogues 6-CF_2-NLX (**5**) and 6-CF_2-NTX (**6**)

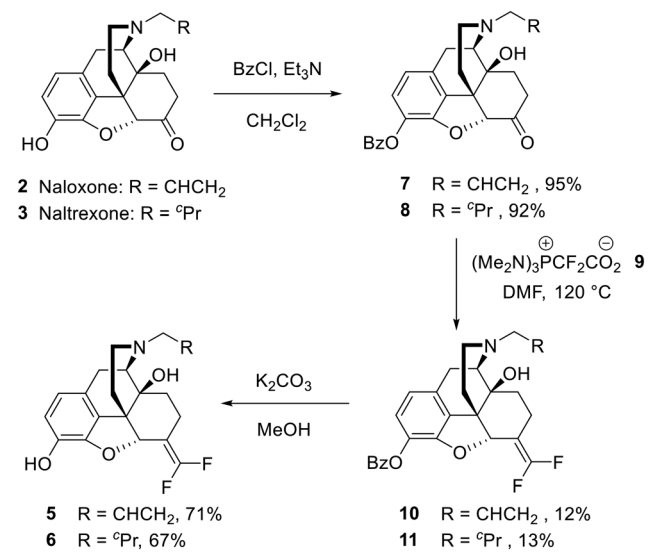

Scheme 1 Synthesis of difluoromethylenated naloxone and naltrexone analogues.

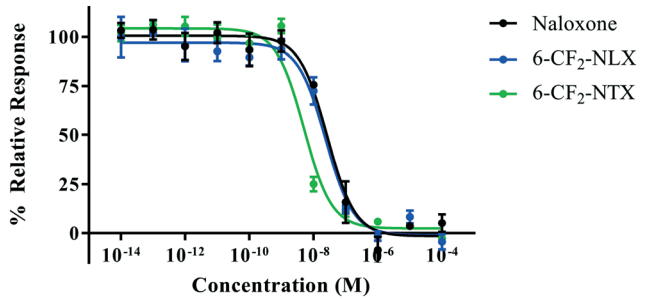

Fig. 6 MOR antagonist potency when challenged with EC_{90} of fentanyl in Lance Ultra cAMP assay. Expressed as mean ± SEM (n = 3).

Table 2 IC_{50} values for three MOR antagonists against EC_{90} challenge of fentanyl

Compound	IC_{50} (nM)	95% CI (nM)
Naloxone	27	13–41
6-CF_2-NLX	24	12–35
6-CF_2-NTX	5.1	2.5–7.6

was achieved by measuring their ability to attenuate a second messenger signal (cAMP) arising from agonism of MORs stably expressed in CHO K1 cells when challenged with an EC_{90} dose of fentanyl. As shown in Fig. 6, concentration–response curves from the cAMP competitive binding assay indicate a very comparable inhibitory profile for both difluorinated analogues relative to the benchmark antagonist naloxone. IC_{50} values depicted in Table 2 show that 6-CF_2-NLX (**5**) is an equipotent MOR antagonist compared to naloxone while the corresponding naltrexone analogue, 6-CF_2-NTX (**6**), exhibits a 5-fold greater potency against fentanyl (IC_{50} = 5 nM *vs.* 27 nM), thus supporting our initial hypothesis regarding the minimal impact of fluorine incorporation on overall antagonist potency.

In vivo MOR antagonist study

The hot plate assay has long been used to test the antinociceptive effects of MOR agonists, including fentanyl.[33] To determine whether the C_6-difluoromethylenated epoxymorphinans, 6-CF_2-NLX (**5**) and 6-CF_2-NTX (**6**), antagonized opioid receptors *in vivo*, we subcutaneously administered either vehicle, 10 mg kg^{-1} naloxone, 10 mg kg^{-1} 6-CF_2-NLX (**5**), or 10 mg kg^{-1} 6-CF_2-NTX (**6**) to C57Bl/6 J mice and monitored the ability of these compounds to block fentanyl-induced anti-nociception in the hot plate assay over time. Given that the serum half-life of naloxone is approximately one hour,[34] this would lead to the possibility of renarcotization within hours of initial treatment. To test the hypothesis that lipophilic MOR antagonists would have longer-lasting effects compared to naloxone hydrochloride, animals were treated with fentanyl (0.4 mg kg^{-1}) at one, eight, and twenty-four hours post treatment. Latency on the hotplate was tested 15 minutes after each individual fentanyl administration. Our results indicate that all MOR antagonists tested blunted the effects of high dose fentanyl at 1 h when compared to vehicle control (Fig. 7A) while at 8 h post-treatment, there were no significant differences in fentanyl MPE between vehicle, naloxone hydrochloride, and 6-CF_2-NLX (**5**) treated groups (Fig. 7B). Contrastingly, 6-CF_2-NTX (**6**) was able to significantly block fentanyl-induced anti-nociception in the hotplate assay at 8 h post-treatment. After 24 h, there was no significant difference between the test groups (Fig. 7C). Overall, these studies served as a critical tool to confirm the retention of full MOR antagonism by C_6-difluorinated epoxymorphinans against fentanyl as the modification of neither naloxone nor naltrexone diminished the acute *in vivo* effects of these established MOR antagonists. However, it remains unclear whether the extended blockade of high dose fentanyl observed for 6-CF_2-NTX is the direct result of fluorine incorporation at the C_6 position or simply an effect of *N*-cyclopropylmethyl substitution[35] and ketone replacement.

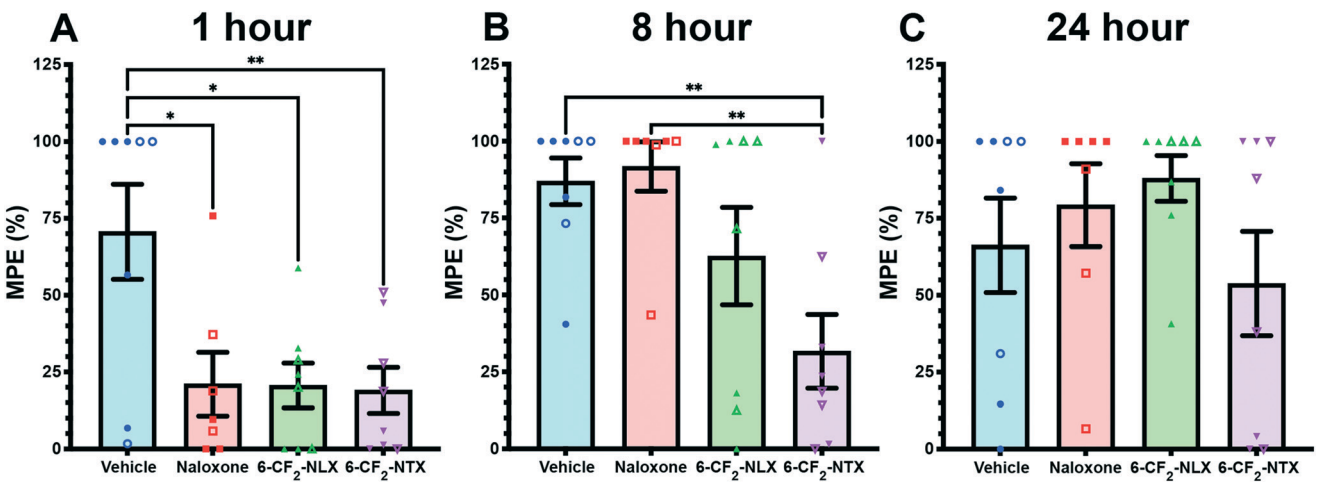

Fig. 7 MOR antagonists decrease fentanyl-induced anti-nociception in the hot plate assay. C57Bl/6 J mice were treated with either 10 mg kg^{-1} of naloxone hydrochloride, 6-CF_2-NLX (**5**) and 6-CF_2-NTX (**6**), or vehicle (10% DMSO, 90% PBS). At (A) 1 h, (B) 8 h, and (C) 24 h post treatment, mice received 0.4 mg kg^{-1} of fentanyl and latency on the hot plate was tested 15 minutes post fentanyl injection. Open symbols are female mice; closed symbols are male mice. * $p < 0.05$, ** $p < 0.01$ one-way ANOVA with Tukey *post-hoc* analysis.

While the argument that 6-CF_2 modification does not enhance the duration of action can be made given the lack of statistical significance observed between naloxone and 6-CF_2-NLX after 8 h, it cannot be definitively concluded as the selection of this later time point may be obscuring the potential efficacy of 6-CF_2-NLX *vs.* naloxone at earlier stages in the assay. Future studies will feature the inclusion of earlier time points (*e.g.*, 2–4 h) as well as additional direct comparator controls (naltrexone and/or nalmefene) to provide a more complete assessment of the potential extended antagonistic effects of these compounds.

In summary, we have prepared novel difluoromethylenated MOR antagonist analogs 6-CF_2-NLX (**5**) and 6-CF_2-NTX (**6**) in an attempt to address the threat of renarcotization posed by synthetic opioids, such as fentanyl. *In silico* modeling of Log P and pharmacokinetics predicted that these compounds would possess increased lipophilicity and enhanced circulatory half-life in humans compared to naloxone, the current standard of treatment for opioid intoxication rescue and reversal. C_6-difluoromethylenation of the classical epoxymorphinan-based MOR antagonist core structure, accomplished *via* a previously described decarboxylative Wittg olefination, seemed to be well tolerated as both analogues maintained low nanomolar *in vitro* potency against an EC_{90} fentanyl challenge and displayed comparable acute *in vivo* efficacy. 6-CF_2-NTX (**6**) appeared to possess the most favorable drug-like attributes *in silico* in order to render it a longer lasting, and more potent MOR antagonist due its predicted higher Log P, faster redistribution and increased residence in the central compartment, as well as higher accumulation in the CNS compared to 6-CF_2-NLX (**5**) and naloxone. While this compound demonstrated significant *in vivo* blockade of high dose fentanyl 8 h after administration in C57Bl/6 J mice, it is not clear whether this effect is directly related to the incorporation of a 1,1-difluoroolefin at the C_6 position. As a result of this preliminary data, further investigation into the potential extended antagonistic effects of these compounds is warranted. Expanded SAR development to determine the effect of fluorination at other positions in the epoxymorphinan scaffold is also planned. Additionally, oximetry studies to probe these compounds for both acute and longer-lasting protection against fentanyl-induced respiratory depression as well as a full *in vivo* pharmacokinetic workup are planned and will be reported in due course.

Conflicts of interest

There is no conflict of interest to declare.

References

1 T. H. Stanley, T. D. Egan and H. Van Aken, A Tribute to Dr. Paul A. J. Janssen: Entrepreneur Extraordinaire, Innovative Scientist, and Significant Contributor to Anesthesiology, *Anesth. Analg.*, 2008, **106**, 451–462.

2 T. H. Stanley, The Fentanyl Story, *J. Pain*, 2014, **15**, 1215–1226.

3 H. J. M. Lemmens, Pharmacokinetic-Pharmacodynamic Relationships for Opioids in Balanced Anaesthesia, *Clin. Pharmacokinet.*, 1995, **29**, 231–242.

4 B. Fischer, C. Russell, Y. Murphy and P. Kurdyak, Prescription opioids, abuse and public health in Canada: is fentanyl the new centre of the opioid crisis?, *Pharmacoepidemiol. Drug Saf.*, 2015, **24**, 1334–1336.

5 G. T. T. Helmerhorst, T. Teunis, S. J. Janssen and D. Ring, An epidemic of the use, misuse and overdose of opioids and deaths due to overdose, in the United States and Canada, *Bone Jt. J.*, 2017, **99**, 856–864.

6 K. M. C. Verhamme and A. M. Bohnen, Are we facing an opioid crisis in Europe?, *Lancet Public Health*, 2019, **4**, e483–e484.

7 J. Mounteney, I. Giraudon, G. Denissov and P. Griffiths, Fentanyls: Are we missing the signs? Highly potent and on the rise in Europe, *Int. J. Drug Policy*, 2015, **26**, 626–631.

8 J. G. Bovill and P. S. Sebel, Pharmacokinetics of High-Dose Fentanyl, *Br. J. Anaesth.*, 1980, **52**, 795–801.

9 E. D. Kharasch, Opioid Half-lives and Hemlines: The Long and Short of Fashion, *Anesthesiology*, 2015, **122**, 969–970.

10 G. S. Murphy, J. W. Szokol, M. J. Avram, S. B. Greenberg, J. H. Marymont, T. Shear, K. N. Parikh, S. S. Patel and D. K. Gupta, Intraoperative Methadone for the Prevention of Postoperative Pain: A Randomized, Double-blinded Clinical Trial in Cardiac Surgical Patients, *Anesthesiology*, 2015, **122**, 1112–1122.

11 R. B. Moss and D. J. Carlo, Higher doses of naloxone are needed in the synthetic opioid era, *Substance Abuse: Treatment, Prevention, and Policy*, 2019, **14**, 6.

12 R. Rzasa Lynn and J. L. Galinkin, Naloxone dosage for opioid reversal: current evidence and clinical implications, *Ther. Adv. Drug Saf.*, 2017, **9**, 63–88.

13 S. F. J. Clarke, Naloxone in opioid poisoning: walking the tightrope, *Emerg. Med. Int.*, 2005, **22**, 612–616.

14 H. L. Sun, Naloxone-Precipitated Acute Opioid Withdrawal Syndrome After Epidural Morphine, *Anesth. Analg.*, 1998, **86**, 544–545.

15 P. D. Kanof, L. Handelsman, M. J. Aronson, R. Ness, K. J. Cochrane and K. J. Rubinstein, Clinical characteristics of naloxone-precipitated withdrawal in human opioid-dependent subjects, *J. Pharmacol. Exp. Ther.*, 1992, **260**, 355–363.

16 P. Shah and A. D. Westwell, The role of fluorine in medicinal chemistry, *J. Enzyme Inhib. Med. Chem.*, 2008, **22**, 527–540.

17 M. Meanwell, B. Adluri, S. Yuan, Z. Yuan, J. Newton, P. Prevost, M. B. Nodwell, Chadron M. Friesen, P. Schaffer, R. E. Martin and R. Britton, Direct heterobenzylic fluorination, difluorination and trifluoromethylthiolation with dibenzenesulfonamide derivatives, *Chem. Sci.*, 2018, **9**, 5608–5613.

18 N. A. Meanwell, Synopsis of Some Recent Tactical Application of Bioisosteres in Drug Design, *J. Med. Chem.*, 2011, **54**, 2529–2591.

19 P. M. Weintraub, A. K. Holland, C. A. Gates, W. R. Moore, R. J. Resvick, P. Bey and N. P. Peet, Synthesis of 21,21-Difluoro-3β-hydroxy-20-methylpregna-5,20-diene and 5,16,20-Triene as potential inhibitors of steroid C17(20) lyase, *Bioorg. Med. Chem.*, 2003, **11**, 427–431.

20 N. A. Meanwell, Fluorine and Fluorinated Motifs in the Design and Application of Bioisosteres for Drug Design, *J. Med. Chem.*, 2018, **61**, 5822–5880.
21 J. Zheng, J. Cai, J.-H. Lin, Y. Guo and J.-C. Xiao, Synthesis and decarboxylative Wittig reaction of difluoromethylene phosphobetaine, *Chem. Commun.*, 2013, **49**, 7513–7515.
22 M. L. Quan, P. Y. S. Lam, Q. Han, D. J. P. Pinto, M. Y. He, R. Li, C. D. Ellis, C. G. Clark, C. A. Teleha, J.-H. Sun, R. S. Alexander, S. Bai, J. M. Luettgen, R. M. Knabb, P. C. Wong and R. R. Wexler, Discovery of 1-(3‘-Aminobenzisoxazol-5′-yl)-3-trifluoromethyl-N-[2-fluoro-4- [(2′-dimethylaminomethyl)-imidazol-1-yl]phenyl]-1H-pyrazole-5-carboxyamide Hydrochloride (Razaxaban), a Highly Potent, Selective, and Orally Bioavailable Factor Xa Inhibitor, *J. Med. Chem.*, 2005, **48**, 1729–1744.
23 C. Hansch, A. Leo, S. B. Mekapati and A. Kurup, QSAR and ADME, *Bioorg. Med. Chem.*, 2004, **12**, 3391–3400.
24 F. Lombardo, R. S. Obach, M. Y. Shalaeva and F. Gao, Prediction of Volume of Distribution Values in Humans for Neutral and Basic Drugs Using Physicochemical Measurements and Plasma Protein Binding Data, *J. Med. Chem.*, 2002, **45**, 2867–2876.
25 J. H. Lin and A. Y. Lu, Role of pharmacokinetics and metabolism in drug discovery and development, *Pharmacol. Rev.*, 1997, **49**, 403–449.
26 W. M. Pardridge, Transport of small molecules through the blood-brain barrier: biology and methodology, *Adv. Drug Delivery Rev.*, 1995, **15**, 5–36.
27 V. A. Levin, Relationship of octanol/water partition coefficient and molecular weight to rat brain capillary permeability, *J. Med. Chem.*, 1980, **23**, 682–684.
28 W. M. Pardridge, CNS Drug Design Based on Principles of Blood-Brain Barrier Transport, *J. Neurochem.*, 1998, **70**, 1781–1792.
29 M. Concheiro, R. Chesser, J. Pardi and G. Cooper, Postmortem Toxicology of New Synthetic Opioids, *Front. Pharmacol.*, 2018, **9**, 1210.
30 S. A. Peters, *Physiologically-Based Pharmacokinetic (PBPK) Modeling and Simulations*, 2012, DOI: 10.1002/9781118140291.
31 H. M. Jones and K. Rowland-Yeo, Basic Concepts in Physiologically Based Pharmacokinetic Modeling in Drug Discovery and Development, *CPT: Pharmacometrics Syst. Pharmacol.*, 2013, **2**, 63.
32 S. Béni, G. Tóth, B. Noszál and S. Hosztafi, Preparation of benzoate esters of morphine and its derivatives, *Monatsh. Chem.*, 2012, **143**, 1431–1440.
33 J. G. Williams, J. H. Brown and B. J. Pleuvry, Alfentanil: a study of its analgesic activity and interactions with morphine in the mouse, *Br. J. Anaesth.*, 1982, **54**, 81–85.
34 S. H. Ngai, B. A. Berkowitz, J. C. Yang, J. Hempstead and S. Spector, Pharmacokinetics of naloxone in rats and in man: basis for its potency and short duration of action, *Anesthesiology*, 1976, **44**, 398–401.
35 E. F. Hahn, J. Fishman and R. D. Heilman, Narcotic antagonists. 4. Carbon-6 derivatives of N-substituted noroxymorphones as narcotic antagonists, *J. Med. Chem.*, 2002, **18**, 259–262.

